Polyhedron 190 (2020) 114765

Contents lists available at ScienceDirect

Polyhedron

journal homepage: www.elsevier.com/locate/poly

Synthesis, structure, and electronic properties of late first-row transition metal complexes of fluorinated alkoxides and aryloxides

Jessica K. Elinburg, Linda H. Doerrer *

Department of Chemistry, Boston University, Boston, MA 02215, USA

ARTICLE INFO

Article history:
Received 18 June 2020
Accepted 19 August 2020
Available online 27 August 2020

Keywords:
Electronic structure
Coordination geometry
Transition metal
Aryloxide
Alkoxide
Fluorinated

ABSTRACT

The synthesis, structure, and electronic properties of several series of late first-row transition metal complexes stabilized by highly-fluorinated alkoxide and aryloxide (OR^F) ligands, including partially fluorinated OAr' ($3,5\text{-}OC_6H_3(CF_3)_2)^-$ and fully fluorinated OAr^F ($OC_6F_5)^-$, perfluoro-^{t}butoxide ($OC_4F_9)^-$, and perfluoropinacolate, denoted as pin^F, $(\{OC(CF_3)_2\}_2)^{2-}$ are described herein. Compared to their protio counterparts, the powerful electron-withdrawing nature of these fluorinated ligands makes them considerably less basic and some syntheses may be conveniently carried out in aqueous media when the metal redox chemistry is compliant. Additionally, the decreased propensity of these ligands to form bridging complexes reduces the number of dimeric or polymeric extended structures, leading to monomeric systems whose corresponding protio analogs may not be synthetically achieved. As pseudo-halogens, these ligands have been found to be electronically similar to fluoride (F^-), and in several cases, spectroscopic characterization of their corresponding metal complexes has revealed high-spin electronic configurations, justifying their description as medium field ligands. Furthermore, interactions between O/F atoms on the ligand and counter-cations such as K^+ and Tl^+ play a key structural role, influencing the solubility and solid-state nuclearity or geometry of the complexes.

Contents

1. Introduction

Understanding the electronic structure and reactivity of transition metal ions surrounded by an O-donor environment has long been a goal of inorganic chemists in order to model the structure and/or catalytic activity of enzyme active sites, such as the oxygen evolving complex (OEC) of photosystem II (PSII) [1,2], industrially-relevant M_xO_y catalysts [3], and zeolite frameworks [4–6]. Due to the challenges of short lifetimes and isolation limitations, understanding the mechanisms by which these enzymatic or heterogeneous processes occur is challenging. Thus, the synthetic pursuit

* Corresponding author.
E-mail address: doerrer@bu.edu (L.H. Doerrer).

https://doi.org/10.1016/j.poly.2020.114765
0277-5387/

of transition metal complexes supported by alkoxide and aryloxide (OR) ligands is of great interest. Within the realm of OR ligands, the Brønsted basicity of the oxygen lone pair combined with the limited steric bulk effected by a single substituent leads to the pervasive formation of μ-OR-bridged structures. These multimeric systems contain coordinatively-saturated metal centers and, consequently, abated reactivity [7].

To date, examples of discrete mononuclear $[M(OR)_n]^{m-}$ complexes are relatively limited. One strategy to isolate monomeric metal alkoxide complexes has been the utilization of sterically bulky OR ligands that can prevent bridging, *e.g.* ligands with a steric profile larger than *t*-butoxide (OC_4H_9) can result in the formation of monomeric $[M(OR)_n]^{m-}$ complexes (Fig. 1) [8]. The Power [9–14], Wolczanski [15–18], Nocera [19–22], and Groysman [23–27] groups have employed this steric strategy extensively and investigated both heteroleptic and homoleptic Mn, Cr, and Fe complexes featuring symmetrically-substituted bulky alkoxide/siloxide ligands such as tritox (OC^tBu_3) [9–12,15–17], silox (OSi^tBu_3) [18], ($OCCy_3$) [13], and ($OCPh_3$) [14], as well as asymmetric systems such as ditox (OC^tBu_2Me) [19–22], (OC^tBu_2Ph) [23,25,27], and the exceptionally bulky ($C^tBu_2(C_6H_3Ph_2)$) (Figure 1, adapted from Grass et al. [8]) [24,26].

Another strategy to circumvent bridging behavior is to decrease the basicity of the ligand by fluorination. As shown in Fig. 2(a), fluorinated alcohols are considerably more acidic than their protio counterparts [28–33], and, consequently, their conjugate bases, are much less basic. This reduced basicity decreases the propensity of highly-fluorinated alkoxide and aryloxide (OR^F) ligands to bridge, instead forming terminal M-OR^F linkages that promote the formation of monomeric compounds. The resulting low-coordinate, monomeric compounds can have open coordination sites for substrate binding during reactivity and catalysis. In addition to the propensity of OR^F ligands to produce monomeric complexes, perfluorination of the C—H bonds in OR^F ligands decreases the susceptibility of oxidative ligand degradation, due to the relative strength of C—F bonds (117 kcal/mol) versus C—H bonds (99 kcal/mol) [34], and thereby stabilizing the C—F based system under highly-oxidizing environments.

The comparative basicity of highly-fluorinated ligands versus their protio analogs in forming terminal versus bridging linkages is manifest in the isolation of a series of heteroleptic Cu(II) complexes featuring both (OC_4H_9) and (OC_4F_9) ligands by Purdy and coworkers (Fig. 2(b)) [35]. In the Cu(II) tetramer shown, despite the addition of an excess of perfluoro-*t*-butanol to the reaction mixture, six *t*-butoxide ligands bridge consecutive metal centers, while a perfluoro-*t*-butoxide ligand caps each end of the complex.

There are alternative methods to reduce the donor capacity of the oxygen atom in alkoxide-type ligands, such as use of a boroxide ligand, O-BR_2, in which the three-coordinate boron atom attracts the oxygen lone pairs [36–38]. These compounds have been reviewed elsewhere and will not be discussed further here [39].

Over the past 15 years, the Doerrer group has developed an extensive collection of over 50 late transition metal complexes supported by highly fluorinated ligands including OAr^F $(OC_6F_5)^-$ [40–46], OAr' $(OC_6H_3(CF_3)_2)^-$ [40–46], perfluoro-*t*butoxide $(OC_4F_9)^-$ [43,47,48], and perfluoropinacolate, denoted as pin^F, $(\{OC(CF_3)_2\}_2)^{2-}$ (Table 1) [49–51]. Herein, the synthesis and properties of divalent and trivalent Fe-, Co–, Ni-, Cu-, and Zn-OR^F complexes with various counter ions will be reviewed, with emphasis on synthetic approaches, metal coordination numbers and geometries, and initial reactivity observations. This work complements the recent overview of the O_2 reactivity of $\{Cu^IOR^F\}$ complexes recounted by Brazeau et al. [52]. Analysis of these late 3*d* systems demonstrates the success of our initial compositional hypotheses as well as indicates unexpected behavior and electronic structures of these first-row transition metal complexes stabilized by an all-O-donor ligand environment.

2. Synthesis of $[M(OR^F)_n]^{m-}$ complexes

Generally speaking, complexes were prepared by typical metathesis reactions of the corresponding metal and ligand salts, although, in several cases, the synthesis of $[M(OR^F)_n]^{m-}$ complexes proved usefully sensitive to ligand/metal ratio, metal source, and/or reaction conditions. While in many cases, syntheses of metal complexes of the corresponding non-fluorinated alkoxide/aryloxide ligands result in the formation of polymeric μ-OR-bridged structures [7], in the fluorinated realm, simply adjusting the M:OR^F ratio conveniently allows for the selective formation of monomeric/dimeric complexes [44–46]. Furthermore, encapsulation of K^+ counter-ions with 18-crown-6 (18C6) or counter-ion exchange of K^+ in these $[M(OR^F)_n]^{m-}$ complexes with quaternary R_4P^+ or R_4N^+ salts has resulted in an extensive library (Table 1) of $[M(OR^F)_n]^{m-}$ salts. This library has allowed our group to investigate the role that counter-ions, including Lewis-acidic K^+ and Tl^+, play in determining the structure and solubility of highly-fluorinated metal complexes.

As previously discussed, one of the key advantages of OR^F ligands is the ability to readily prepare monomeric compounds. The majority of complexes presented herein are monomeric species, but in some cases, the formation of dimers **4** [44], **7** [46], **14**

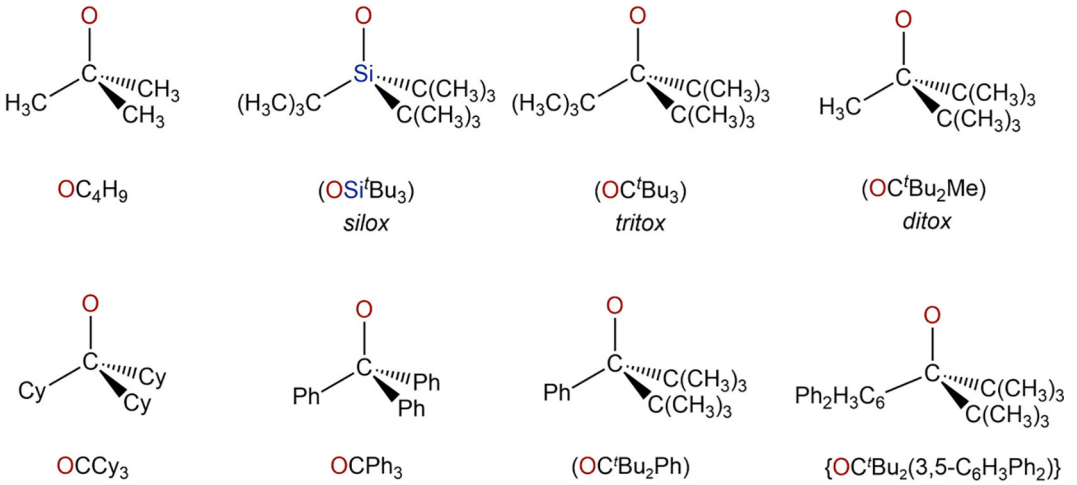

Fig. 1. Commonly used bulky alkoxide ligands. Adapted from Grass et al. [8].

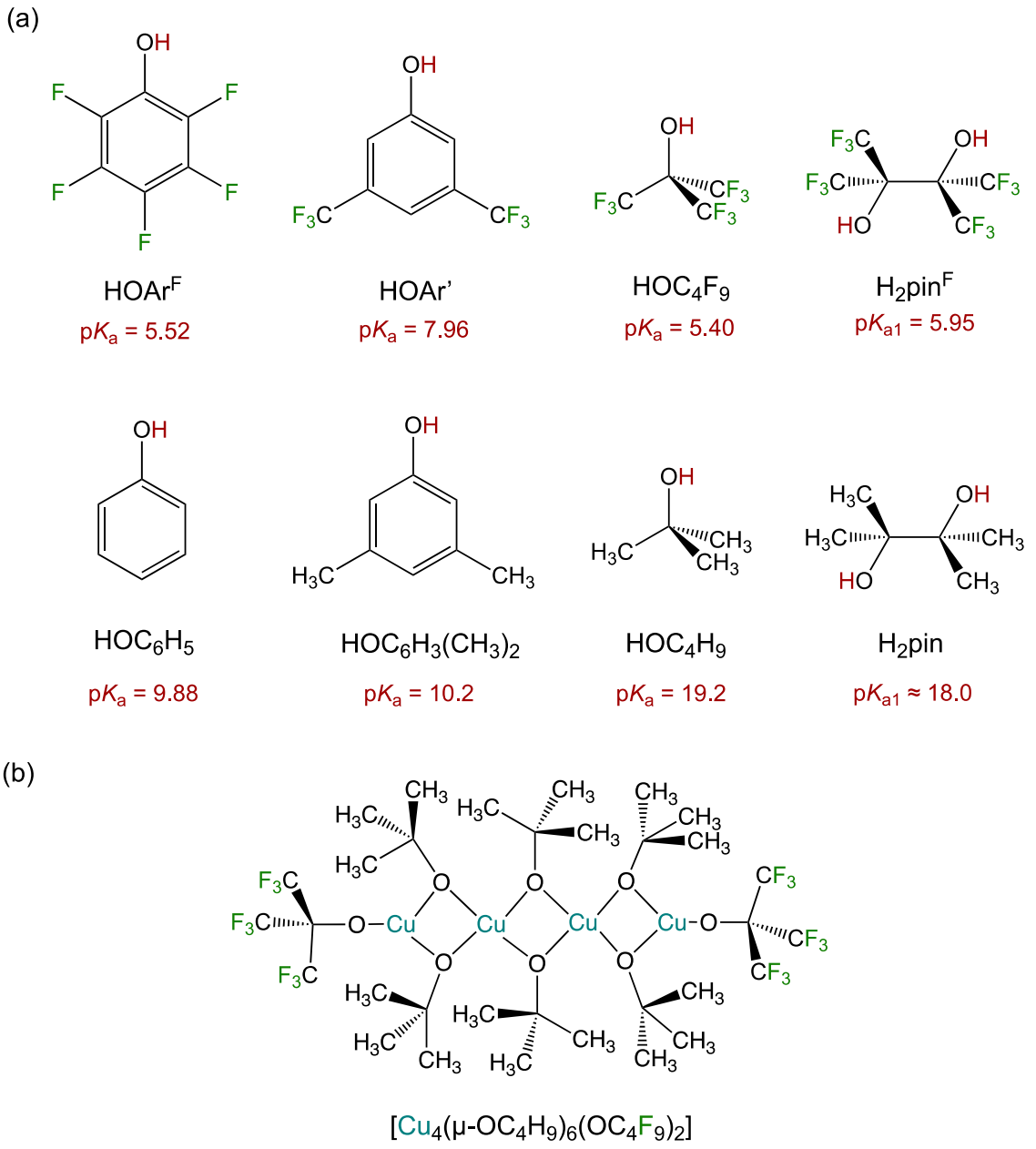

Fig. 2. (a) Comparison of pK_a values for fluorinated and non-fluorinated alkoxides and aryloxides; (b) Bridging versus terminal alkoxide ligands in Purdy's Cu tetramer [34].

[46], and **19** [45] was also possible when the metal to ligand ratio was sufficiently increased. Additionally, early work in the Doerrer Group directly investigated the effect of fluorination on complex nuclearity by synthesizing analogous Co and Cu complexes with perhydro- and perfluorophenoxide ligands [40]. As shown in Scheme 1, reaction of the corresponding divalent metal salt (Co or Cu) with four equivalents of KOC_6H_5 yielded alkoxide-bridged $[(OPh)_2M(II)(\mu_2\text{-}OPh)_2M(II)(OPh)_2]^{2-}$ dimers. Analogous reactions of Co(II) or Cu(II) with four equivalents $KOAr^F$ yielded monomeric $[M(OAr^F)_4]^{2-}$ complexes (Co, **5** and Cu, **10**). The metal-to-ligand synthetic ratio can also be used to shift the equilibrium and force otherwise unobtainable coordination environments. In 2013, Zadrozny and coworkers demonstrated that a monomeric Co(II) perhydrophenoxide complex could be isolated by altering reaction stoichiometry [55]. By employing an excess of ligand, the first monomeric $[Co(OC_6H_5)_4]^{2-}$ moiety was crystallographically characterized, corroborating other examples of equilibria shifted by increasing amounts of ligand [40,47] and disproving initial speculation that such alkoxides exclusively formed polymeric structures [7,40].

2.1. Complexes with OAr^F

The syntheses of {M(OAr^F)}-containing **1**–**11** (OAr^F = $(OC_6F_5)^-$), are shown in Schemes 2 (K^+), 3 (Tl^+), and 4 (H^+), separated by the counter cation of the starting phenolate. Four-coordinate OAr^F complexes of divalent Fe, Co, Cu, and Zn were synthesized by reaction of corresponding divalent metal salt with four equivalents of $KOAr^F$ ligand salt and either the addition of 18C6 as a K^+ encapsulating agent (**1**, **5a**, **10a**, **11a-b**) (Scheme 2) or subsequent counter-ion exchange with Ph_4P^+ (**6**, **10c**) or Me_4N^+ (**5c**) (Scheme 3). Interestingly, the synthesis of Zn analogs **11a-b** proved particularly sensitive to the Zn:OAr^F ratio employed, resulting in incomplete K^+ encapsulation by 18C6 when slightly less than four equivalents of (OAr^F) ligand were added (**11b**). This stoichiometric sensitivity is not observed for OAr^F complexes of other the first-row metals.

Table 1
Summary of $[M(OR^F)_n]^{m-}$ complexes and their geometries.

Four-coordinate complexes

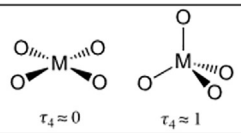

Square planar (τ_4 < 0.5)[53]

Complex	A	τ_4	Ref.	
$A_2[Fe(pin^F)_2]$	$\{K(DME)_2\}^+$	0.00	45	**26a**
	Me_4N^+	0.00	46	**26b**
$A_2[Co(pin^F)_2]$	$\{K(DME)_2\}^+$	0.00	45	**27a**
	Me_4N^+	0.40(1)	46	**27b**
	Bu_4N^+	0.00	46	**27c**
$A[Co(pin^F)_2]$	Me_4N^+	0.03	47	**28**
$[(PPh_3)_2Ni(OAr^F)_2]$		0.00	38	**9**
$[(PPh_3)_2Ni(OAr')_2]$		0.09	38	**16**
$A_2[Ni(pin^F)_2]$	$\{K(DME)_2\}^+$	0.00	46	**30a**
	Me_4N^+	—	46	**30b**
$A_2[Cu(OAr^F)_4]$	$\{K(18C6)\}^+$	—	36	**10a**
	Tl^+	0.19(2)	36, 37	**10b**
	Ph_4P^+	0.00	36	**10c**
	Bu_4N^+	0.00	36	**10d**
	Et_3NH^+	0.00	36	**10e**
$A_2[Cu(OAr')_4]$	$\{K(18C6)\}^+$	0.00	36	**17a**
	Tl^+	0.19	36, 37	**17b**
$A_2[Cu(pin^F)_2]$	K^+	0.00	46	**31a**
	$\{K(DME)_2\}^+$	0.00	46	**31b**
	Me_4N^+	0.00	46	**31c**

Tetrahedral (τ_4 > 0.5)[53]

Complex	A	τ_4	Ref.	
$A_2[Fe(OAr^F)_4]$	$\{K(18C6)\}^+$	0.76	40	**1**
$A_2[(OAr^F)_3Fe(\mu_2\text{-}O)Fe(OAr^F)_3]$	$\{K(18C6)\}^+$	0.96	40	**3**
$A_2[Co(OAr^F)_4]$	$\{K(18C6)\}^+$	0.79	36	**5a**
	Tl^+	0.80	36, 42	**5b**
	Me_4N^+	—	36	**5c**
$A_2[Co(OAr^F)_2Cl_2]$	Ph_4P^+	0.91	36	**6**
$A_2[Co(OAr')_4]$	$\{K(18C6)\}^+$	0.87	36	**13a**
	Tl^+	0.47	36, 42	**13b**
	Cp_2Co^+	0.92	36	**13c**
$A[KCo(OC_4F_9)_4]$	$\{K(18C6)\}^+$	0.79	43	**22**
$A_2[Co(Hpfa)_4]$	Me_4N^+	0.64	47	**29**
$A_2[Ni(OAr^F)_4]$	$\{K(18C6)\}^+$	—	39	**8a**
	$\{K(b\text{-}18C6)\}^+$	0.78	39	**8b**
	Tl^+	0.70(8)	39	**8c**
$A_2[Ni(OAr')_4]$	$\{K(18C6)\}^+$	0.76	39	**15**
$A[KNi(OC_4F_9)_4]$	$\{K(18C6)\}^+$	0.75	39, 43	**23**
$A_2[Zn(OAr^F)_4]$	$\{K(18C6)\}^+$	0.82	41	**11a**
	$K^+\{K(18C6)\}^+$	0.82	41	**11b**
	Tl^+	0.72	41	**11c**
$A_2[Zn(OAr')_4]$	$\{K(18C6)\}^+$	0.85	41	**18**
$A_2[(OAr')_2Zn(\mu_2\text{-}OAr')]_2$	$\{K(18C6)\}^+$	0.85	41	**19**
$A_2[Zn(pin^F)_2]$	K^+	0.80	46	**32a**
	$\{K(DME)_2\}^+$	0.64	45	**32b**

Five-coordinate complexes

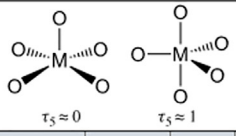

Complex	A	τ_5	Ref.	
Square pyramidal (τ_5 < 0.5)[54]				
$A_2[Fe(OAr^F)_5]$	Ph_4P^+	0.07	40	**2b**
Trigonal bipyramidal (τ_5 > 0.5)[54]				
$A_2[Fe(OAr^F)_5]$	$\{K(18C6)\}^+$	0.84	40	**2a**
	Me_4N^+	0.80	40	**2c**
$A_2[Fe(OAr')_5]$	$\{K(18C6)\}^+$	0.70	40	**12**
$A_2[(OAr^F)_3Fe(\mu_2\text{-}OAr^F)]_2$	$\{K(18C6)\}^+$	0.65	40	**4**
$[(OAr^F)(DME)Co(\mu_2\text{-}OAr^F)_2]$		0.53	42	**7**
$[(OAr')(DME)Co(\mu_2\text{-}OAr')_2]$		—	42	**14**

Three-coordinate complexes

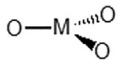

Complex	A	Ref.	
$A[Fe(OC_4F_9)_3]$	$\{K(18C6)\}^+$	43	**20**
$A[Co(OC_4F_9)_3]$	$\{K(18C6)\}^+$	43	**21**
$A[Cu(OC_4F_9)_3]$	$\{K(18C6)\}^+$	43	**24**
$A[Zn(OC_4F_9)_3]$	$\{K(18C6)\}^+$	43	**25**

When multiple crystallographically independent metal centers are present, the average τ value is indicated along with the standard deviation. See above-mentioned references for further information.

In addition to the divalent complexes described above, a series of trivalent Fe-OAr^F complexes has also been prepared from $KOAr^F$. Five-coordinate Fe(III) monomers **2a-c** were prepared by the reaction of $FeBr_3$ with five equivalents of $KOAr^F$ and two equivalents of 18C6 (**2a**) or subsequent counter-ion exchange with Ph_4PBr or Me_4NBr for **2b** and **2c**, respectively. Reducing the metal to ligand ratio from 1:5 to 1:4 resulted in the formation of an Fe(III) dimer **4**, which features two four-coordinate Fe(III) centers bridged by two aryloxide ligands; complex **4** was also prepared by reacting **2a** with PhIO, indicating the formal loss of two aryloxyl radicals

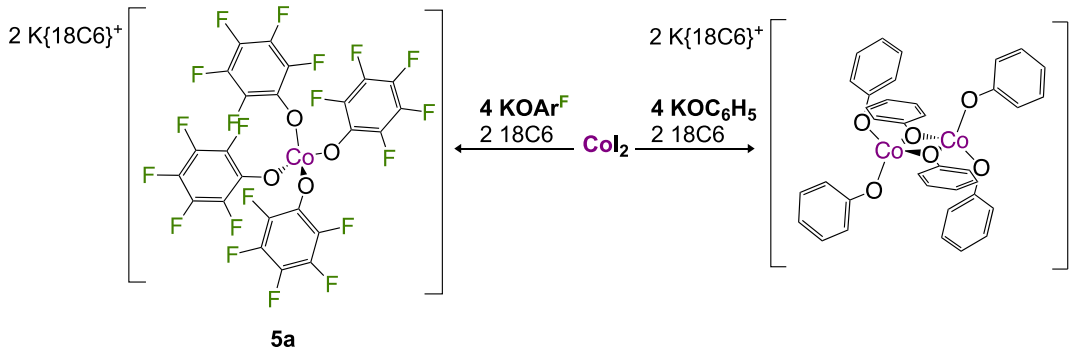

Scheme 1. Comparative syntheses of $[Co(OAr)_4]^{2-}$ complexes with perfluoro versus perhydro phenolate ligands using identical M:OAr ratios.

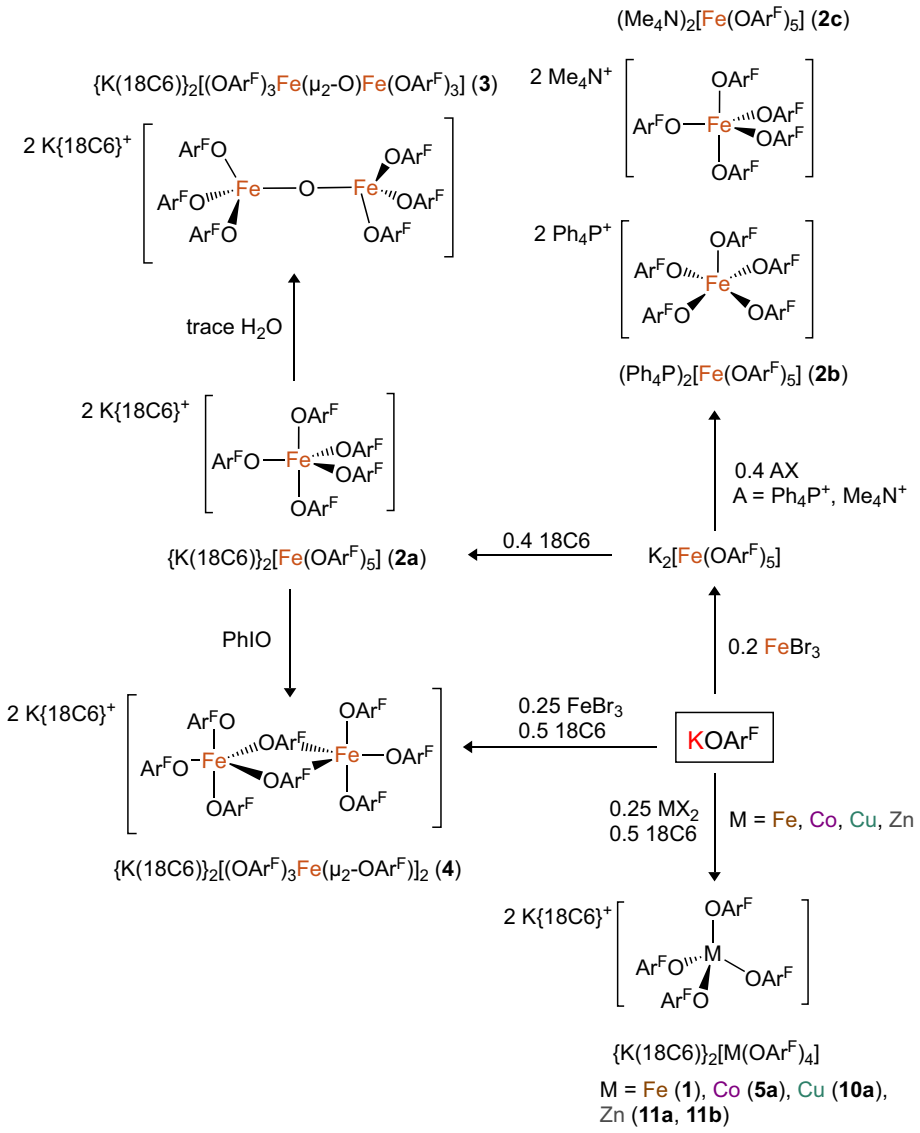

Scheme 2. Synthesis of M-OAr^F complexes with $KOAr^F$.

to produce a final Fe:OAr^F ratio of 1:4 after oxidation. The formation of the four-coordinate Fe(III) $(\mu_2\text{-}O)_2$ bridged dimer **3** resulted from the recrystallization of five-coordinate **2a** from slightly wet solvent, implicating the hydrolysis of two OAr^F ligands per Fe center by adventitious H_2O.

The use of $TlOAr^F$ as the starting phenolate proved especially useful in promoting the formation of M-OAr^F complexes due to the precipitation of highly insoluble TlX salts as byproducts (Scheme 3). Similar to the reactions with $KOAr^F$ described above, Tl-containing $[Tl_2M(OAr^F)_4]$ complexes of Co (**5b**), Cu (**10b**), and Zn (**11c**) were prepared by reaction of corresponding divalent metal salt with four equivalents of $TlOAr^F$ ligand salt; subsequent counter-ion exchange of **5b** and **10c** with Ph_4P^+ or Me_4N^+, respectively, yielded $[M(OAr^F)_4]^{2-}$ complexes of the corresponding

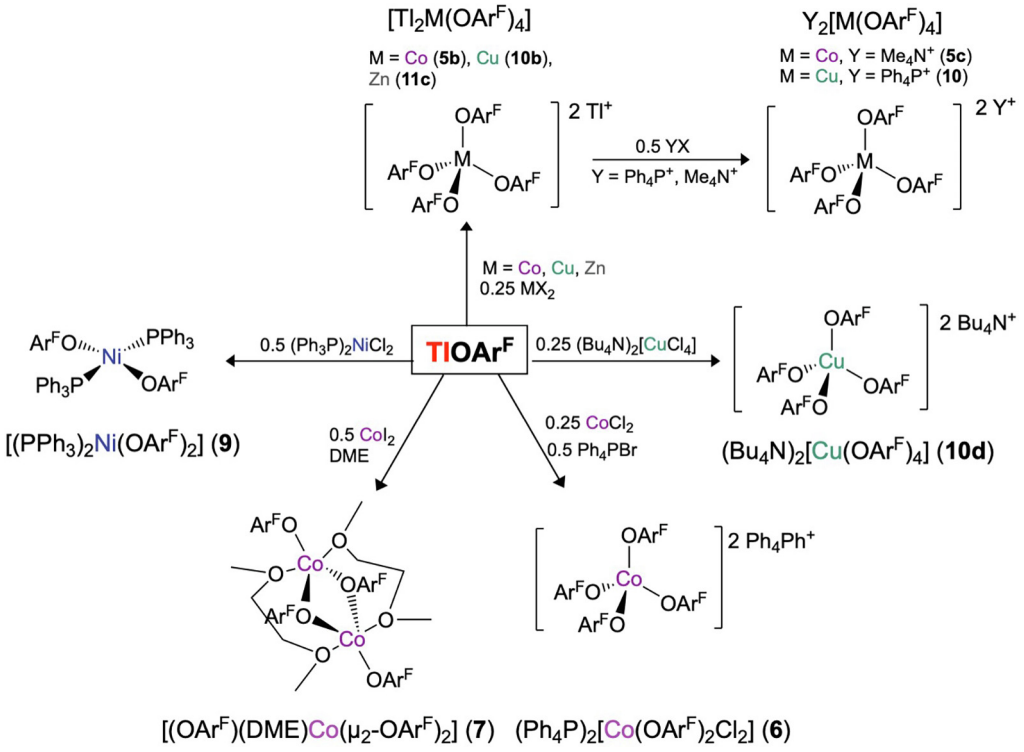

Scheme 3. Synthesis of M-OAr^F complexes with TlOAr^F.

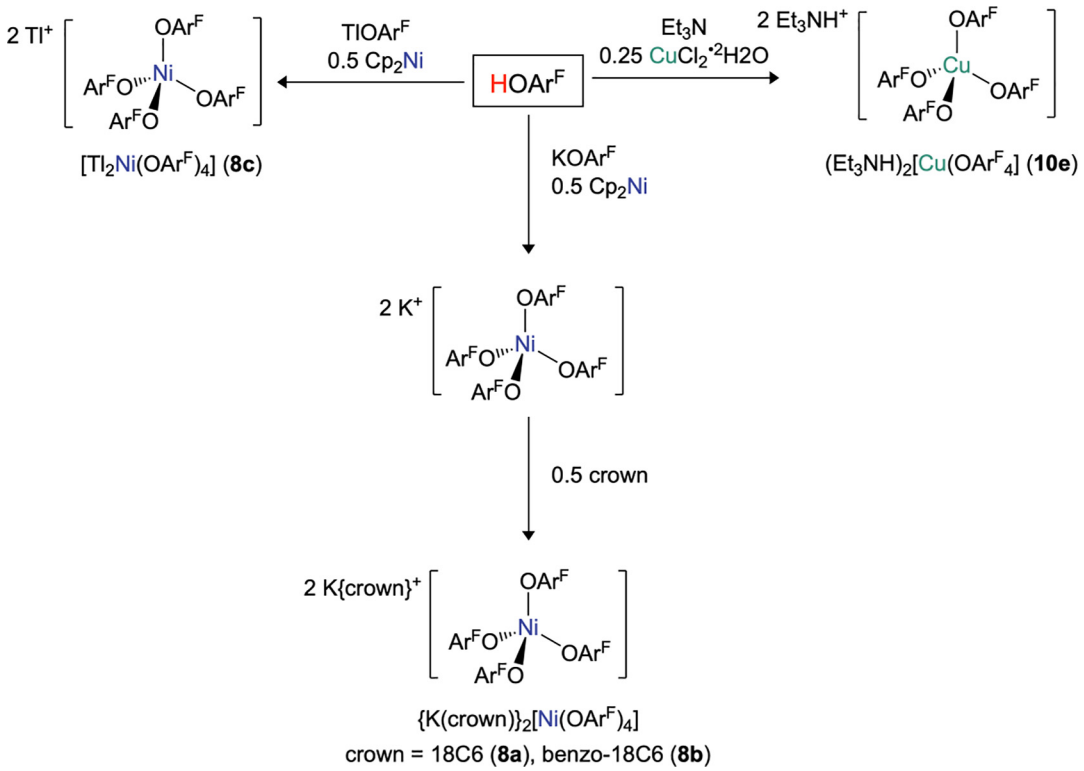

Scheme 4. Synthesis of M-OAr^F complexes with HOAr^F.

quaternary Group 15 salt (**5c**, **10c**). Similarly, reaction of $[Bu_4N]_2[CuCl_4]$ with four equivalents of TlOAr^F resulted in the formation of homoleptic **10d**.

In the Co series **5a-c**, homoleptic coordination was achieved only when CoI_2 was used as the starting metal salt. Reaction of $CoCl_2$ resulted in the formation of four-coordinate heteroleptic

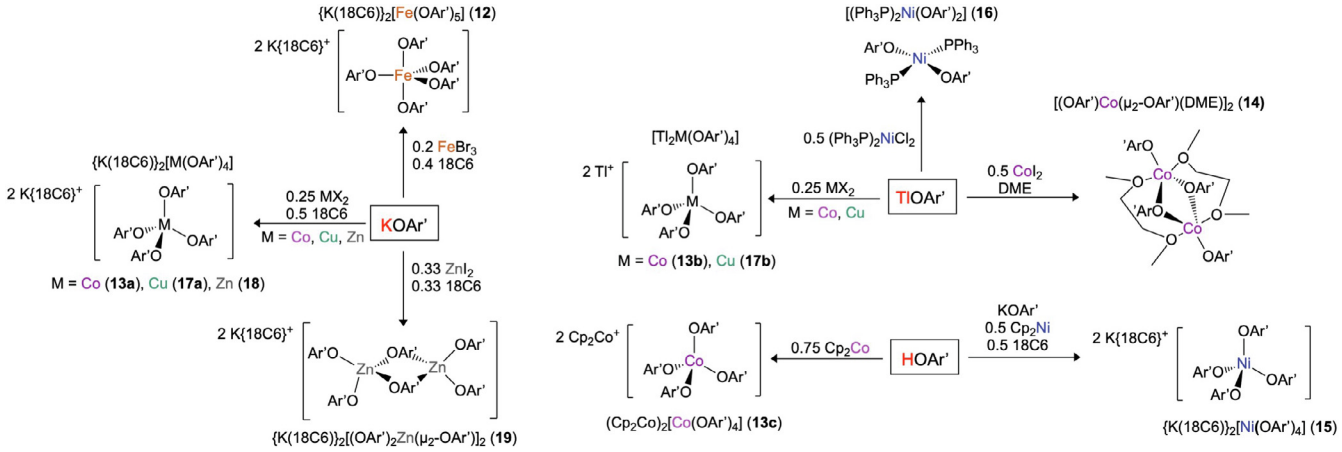

Scheme 5. Synthesis of M-OAr' complexes.

complex **6**, which contains two aryloxide ligands and two chloride ligands; incomplete ligand substitution at the Co center is hypothesized to be the result of strong lattice interactions in $CoCl_2$. Neutral Co dimer **7**, which contains two bridging $(\mu_2\text{-}OAr^F)^-$ ligands, was isolated when a 1:2 ratio of Co:OAr^F was employed. Neutral Ni complex **9**, which binds two equivalents of $(OAr^F)^-$ ligand and two Ph_3P ligands, was prepared when two equivalents of $TlOAr^F$ were reacted with four-coordinate $(PPh_3)_2NiCl_2$.

Finally, several Ni and Cu-OAr^F complexes were prepared beginning with perfluorophenol, $HOAr^F$ (Scheme 4). Interestingly, preparation of homoleptic Ni-OAr^F complexes was possible only when the Ni sources also served as an internal base. When reacted with K/Tl-OAr^F salts, $NiCl_2$ or $NiCl_2$(DME) resulted in incomplete substitution and NiI_2 was reduced to Ni^0. Therefore, Ni-OAr^F complexes (**8a-c**) were synthesized by employing Cp_2Ni as both the metal source and an internal base and adding two equivalents each of $HOAr^F$ and K/Tl-OAr^F ligand salt with subsequent addition of 18C6 (**8a**) or benzo-18C6 (**8b**) as a K^+ encapsulating agent. Additionally, the synthesis of Cu-containing **10e** resulted from the aqueous reaction of a 4:4:1 ratio of $HOAr^F$:Et_3N:$CuCl_2{\cdot}2H_2O$.

2.2. Complexes with OAr'

Syntheses with the {M(OAr')}-containing **12**–**19** (OAr' = $(OC_6H_3(CF_3)_2)^-$) are shown in Scheme 5 and are largely analogous to those with OAr^F. Four-coordinate OAr' complexes of divalent Co, Cu, and Zn (**13a-b, 17a-b, 18**) were synthesized by reaction of the corresponding divalent metal salt with four equivalents of K/Tl-OAr' ligand salt and the addition of 18C6 as a K^+ encapsulating agent (**13a**, **17a**, **18**); similarly, five-coordinate Fe(III)-OAr' complex **12** was prepared when five equivalents of ligand salt were combined with $FeBr_3$. The $[NiX_4]^{2-}$ analog **15** was prepared when Cp_2-Ni was reacted with two equivalents each of HOAr' and KOAr' with subsequent addition of 18C6. Unexpectedly, **13c**, a $[Co(OAr')_4]^{2-}$-containing double-salt with $[Cp_2Co]^+$ counter-ions was prepared when HOAr' and Cp_2Co were combined in a 4:3 ratio. The phenol not only serves as a ligand source via alcoholysis, but also oxidizes Cp_2Co to $[Cp_2Co]^+$, further demonstrating that in general, metathesis with CoI_2 was the most straightforward method for preparing Co(II) complexes.

Similar to the OAr^F analog **9**, neutral heteroleptic Ni complex **16**, was isolated when $(PPh_3)_2NiCl_2$ was reacted with two equivalents of TlOAr'. The formation of μ-OAr'-bridged Co (**14**) and Zn (**19**) dimers was achieved when the metal/ligand ratio was increased. While Zn dimer **19** features two Zn centers, each coordinated to two OAr' ligands, linked by a bis-μ_2-OAr' bridge (Zn:OAr' ratio of 1:3), Co dimer **14** incorporates a single equivalent of DME and OAr' coordinated to each Co center, linked by a bis-μ_2-OAr' bridge (Co:OAr' ratio of 1:2).

2.3. Complexes with OC_4F_9

The synthesis of {M-OC_4F_9}-containing complexes **20**–**25** is shown in Scheme 6. Tris-(OC_4F_9) complexes were obtained for Fe, Co, Cu, and Zn by reacting the corresponding divalent metal salt with three equivalents of KOC_4F_9 and a single equivalent of 18C6 (**20**, **21**, **24**, **25**). In the case of Co and Zn, isolation of a three-coordinate complex was made possible by first forming four-coordinate analog {K(18C6)}[$M(OC_4F_9)_3$(THF)] and placing the complex under vacuum for several hours to remove the bound solvent molecule. While a crystal structure was obtained for {K(18C6)}[$Co(OC_4F_9)_3$], **21**, only the four-coordinate Zn analog {K(18C6)}[$Zn(OC_4F_9)_3$(THF)] was crystallographically characterized, although analytical data supporting the isolation of tris-alkoxide {K(18C6)}[$Zn(OC_4F_9)_3$] were obtained.

Tetrakis-OC_4F_9 complexes, $[M(OC_4F_9)_4]^{2-}$, of Co (**22**) and Ni (**23**) were obtained when four equivalents of KOC_4F_9 were added to the divalent metal salt. Interestingly, **22** and **23** crystallize with only one equivalent of K^+ encapsulated by 18C6, regardless of the amount of crown ether added; accordingly, the crystal structures

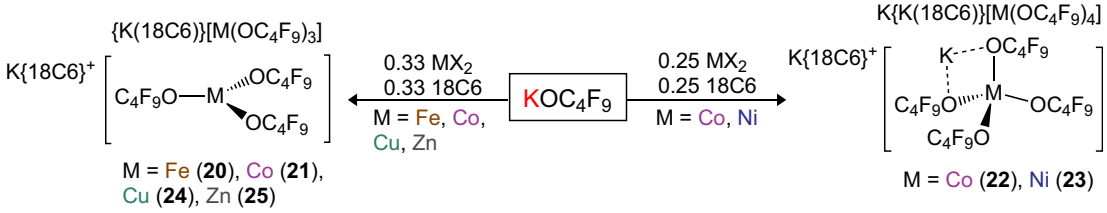

Scheme 6. Synthesis of M-OC_4F_9 complexes.

of **22** and **23** show that the unencapsulated K^+ ion is strongly associated with the O and F atoms of a nearby ligand OC_4F_9 group.

While the isolation of both tris- and tetrakis-OC_4F_9 complexes were possible for Co, only four-coordinate Ni analog $[Ni(OC_4F_9)_4]^{2-}$ was obtained even when the amount of ligand added to reaction mixtures was decreased, despite the comparatively larger ion size of Co(II) versus Ni(II).

2.4. Complexes with pin^F

The syntheses of {M(pin^F)}-containing complexes **26**–**32** (pin^F = $(O(C(CF_3)_2)_2)^{2-}$) are shown in Scheme 7. Divalent $[M(pin^F)_2]^{2-}$ complexes with $\{K(DME)_2\}^+$ counter-ions, Fe (**26a**), Co (**27a**), Ni (**30a**), and Zn (**32b**), were prepared under inert conditions by reacting perfluoropinacol (H_2pin^F), K{N(TMS)$_2$}, and MX_2 in a 2:4:1 ratio and subsequent recrystallization from DME. Under ambient atmosphere, Cu (**31a**) and Zn (**32a**) analogs with unencapsulated K^+ counter-ions were similarly prepared using the same 2:4:1 ligand/base/metal ratio and employing an aqueous base such as KOH or Me_4NOH. The Cu(II) $\{K(DME)_2\}^+$ analog **31b** was prepared via recrystallization of **31a** from DME.

Conveniently, due to the reduced basicity of the pin^F ligand, the aqueous synthesis of divalent Fe, Co, Ni, and Cu $[M(pin^F)_2]^{2-}$ complexes was also possible, although an inert atmosphere proved necessary due to the O_2 sensitivity of the Fe and Co metal centers. In a N_2-filled wet box, M-pin^F complexes with Me_4N^+ counter-ions were prepared with Fe, Co, Ni, and Cu (**26b**, **27b**, **30b**, **31c** respectively) by reacting H_2pin^F, $Me_4NOH \cdot 5H_2O$, and MX_2 in a 2:4:1 ratio. Chemical oxidation of Co(II) in **27b** with $AgPF_6$ under inert atmosphere yielded the exceptional Co(III)-containing **28** [51]. Compared to the classical six-coordinate Werner complexes, square-planar **28** possesses a remarkably low coordination number and does not bind to Lewis bases, preserving its low coordination number. Furthermore, **28** is has an intermediate-spin, $S = 1$, ground state, in a square planar environment; this unique electronic configuration will be further discussed later.

Solutions of **27b** in air were found to convert to **29** over time, which contains four monodentate perfluoroacetone geminal diol $(Hpfa)^{1-}$ ligands connected by four intramolecular hydrogen bonds, formed from the reaction of **28** with reactive oxygen species (ROS). Complex **29** may also be obtained by the addition of hydroxide to solutions of **28** in air, exemplifying the comparative stabilities of Co(II)-containing **27b** and **29** versus Co(III)-containing **28** in air [51].

3. Counter-cation interactions with $\{M(OR^F)_n\}^{m-}$ anions

As detailed above, $[M(OR^F)_n]^{m-}$ complexes have been prepared with a variety of counter-cations, ranging from non-coordinating quaternary Group 15 salts (Me_4N^+, Bu_4N^+, Ph_4P^+) to Lewis acidic Tl^+ and K^+ ions and their 18-crown-6- and DME-encapsulated analogs. In particular, highly fluorinated O-donor ligands, like their more basic perhydro counterparts, are predisposed to forming Lewis acid-base interactions with counter-cations due to the

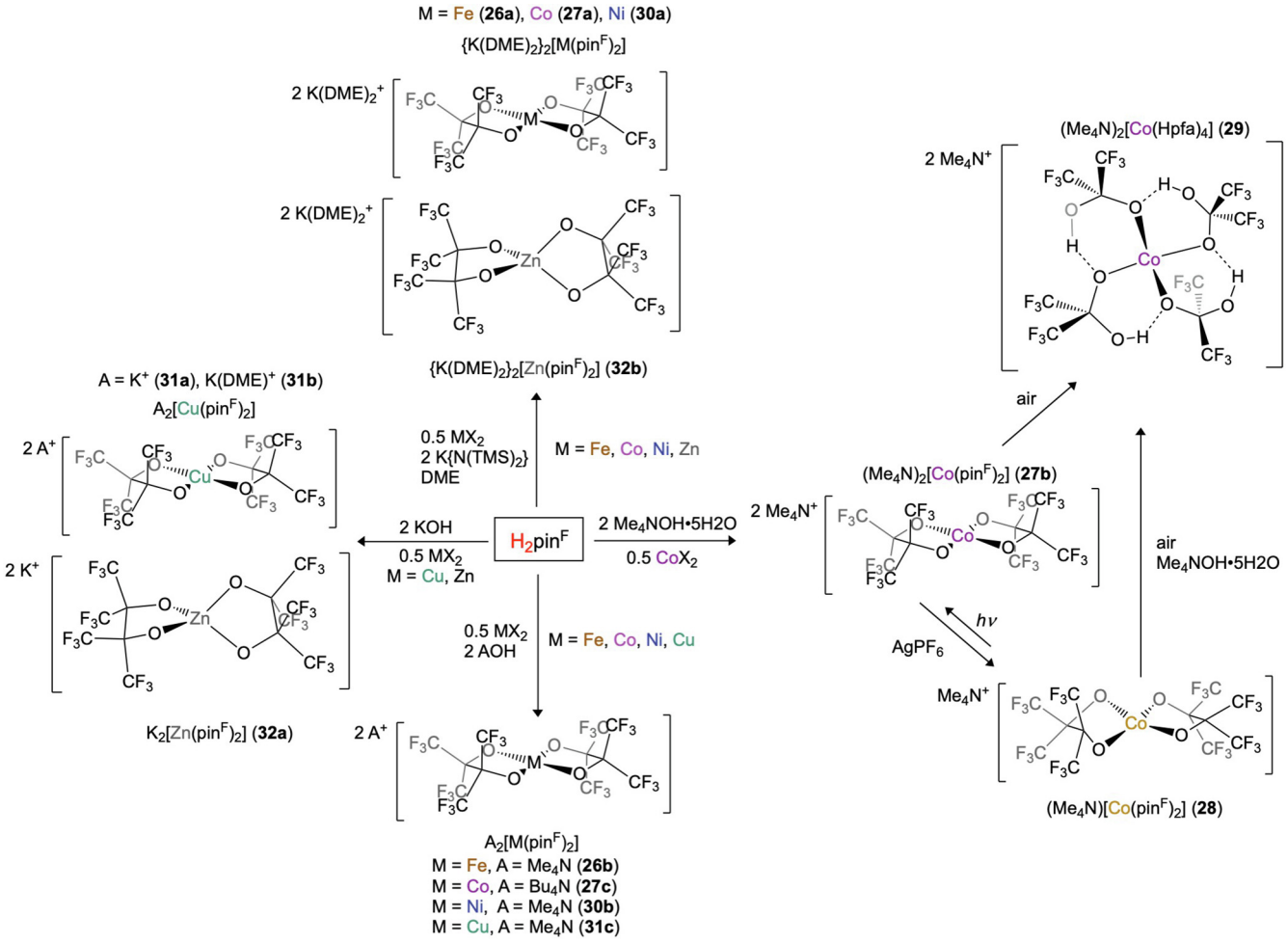

Scheme 7. Synthesis of M-pin^F complexes.

presence of Lewis-basic O and F atoms in the ligand framework. The bridging of alkoxide and aryloxide groups by Lewis acidic cations has contributed significantly to the oligomeric and polymeric structures observed previously [7]. The interactions of the F atoms on OR^F ligands with K^+ and Tl^+ cations have been less well-studied, but significantly affect complex solubility, anion geometry, and nuclearity. The structural motifs observed in of $[M(OR^F)_n]^{m-}$ complexes are summarized in Scheme 8 and discussed below.

3.1. Interactions with K^+ cations

As shown in the left side of Scheme 8, K^+ counter-cations can form inter- and intramolecular K···O and K···F interactions between and within M-OR^F complexes. In general, intermolecular interactions play a key role in the solid state nuclearity of the complexes by forming linkages between alkoxide/aryloxide ligands on adjacent metal centers. Additionally, intramolecular K···O and K···F interactions can affect the geometry of a single metal center, slightly distorting metal environments from their ligand-field driven configurations.

In order to examine the effect of such K^+ interactions on solid-state structures, the Cu- and Zn-pin^F complexes with naked K^+ counter-ions (**31a** and **32a**) and their DME-encapsulated K^+ analogs (**31b** and **32b**) were compared. As shown in Table 2, while the average M···O(pin^F) distance is not significantly different between the naked and encapsulated K^+ analogs for each metal, the number of K···F and K···O interactions is highly dependent on whether there is encapsulation, or not, and on the nature of the counter-ion [48,52,56].

Comparing Cu complexes **31a** and **31b**, naked analog **31a** contains both K···F (3.381 Å) and K···O interactions (2.854 Å) when each K^+ ion is situated in a $\{F_2O_5\}$ coordination environment, but when K^+ is coordinated by DME (**31b**), the number of K···O(pin^F) interactions is reduced to two and no K···F contacts shorter than 4.2 Å are observed. In comparing the Zn complexes **32a** and **32b**, a similar phenomenon is observed. Unencapsulated analog **32a** contains two independent K^+ counter-ions, one with $\{F_3O_5\}$ coordination and the other with $\{F_4O_4\}$ coordination; DME-encapsulated analog **32b** contains two K^+ ions each with $\{F_1O_2\}$ coordination from the ligand in addition to $\{O_4\}$ coordination by the DME solvent molecules. Furthermore, while the geometries of the square-planar Cu-containing **31a** and **31b** are not affected by K···F and K···O interactions, Zn-containing **32a** and **32b** are distorted from their expected tetrahedral geometry (τ_4 = 1) with τ_4 values[54] of 0.80 and 0.64, respectively, due to bridging K^+ interactions and constraints of the resultant five-member chelate ring. Generally, it is expected that naked K^+ ions would interact more strongly with the Zn-pin^F anion than their encapsulated counterparts; thus, the comparative distortions of **32a** and **32b** from perfect tetrahedral geometry remain slightly counterintuitive.

In one particular family, K···F and K···O interactions dominate such that complete K^+ encapsulation by 18C6 is not observed. In particular, four-coordinate $[M(OC_4F_9)_4]^{2-}$ complexes **22** (Co) and

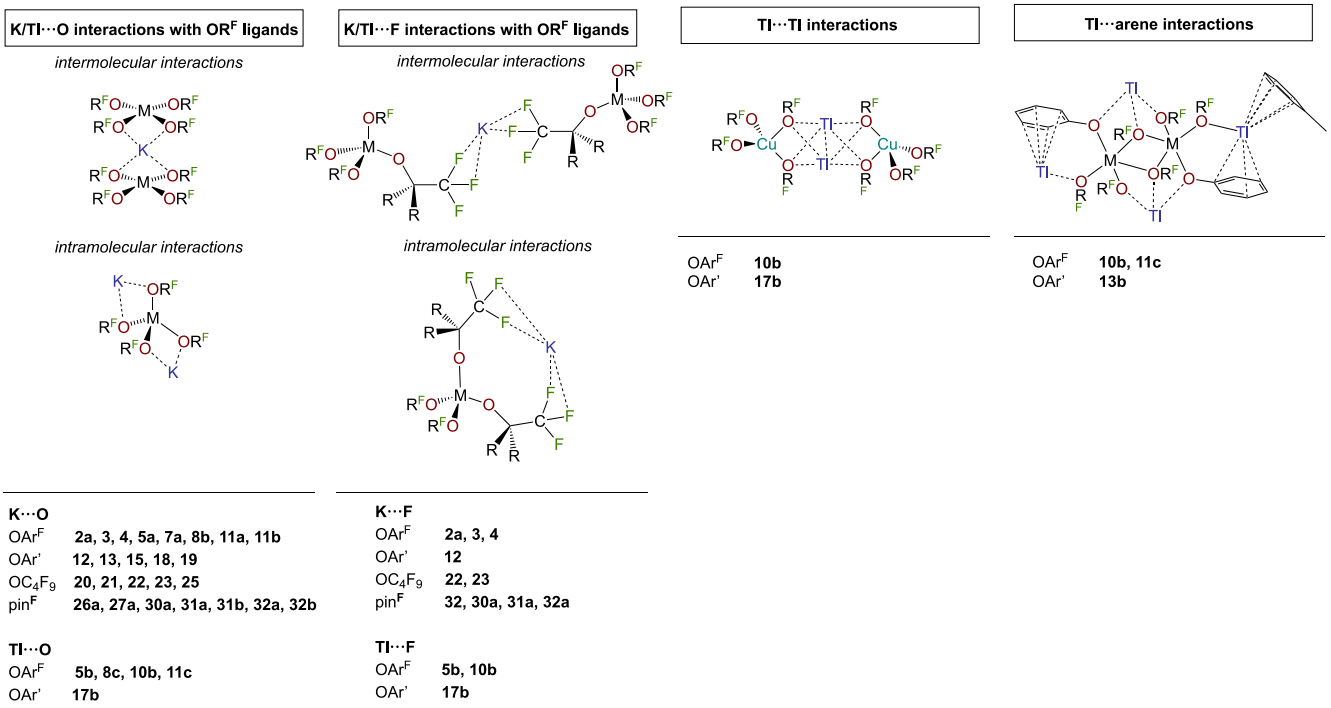

Scheme 8. Summary of K^+ and Tl^+ interactions in $[M(OR^F)_n]^{m-}$ complexes.

Table 2
Comparison of K···O and K···F distances in Cu- and Zn-pin^F complexes.

Compound No.	31a	31b	32a	32b
Average distance (Å)	$K_2[Cu(pin^F)_2]$	$\{K(DME)_2\}_2$ $[Cu(pin^F)_2]$	$K_2[Zn(pin^F)_2]$	$\{K(DME)_2\}_2$ $[Zn(pin^F)_2]$
M···O(pin^F)	1.905(14)	1.916(2)	1.947(14)	1.944(3)
K···O(pin^F)	2.854(16)	2.691(2)	2.762(17), 2.823(17)	2.756(4)
K···F	3.0165(17)	—	2.955(15), 2.920(14)	3.052(8)
τ_4 [54]	0.0	0.0	0.80	0.64

23 (Ni) crystallize with two K^+ counter-ions, but only one K^+ is coordinated to 18C6, no matter how many equivalents of crown ether are added (Fig. 3). In these two examples, the unencapsulated K^+ is coordinated to nine O and F atoms on the perfluoro-*t*-butoxide ligand with $\{O_3F_6\}$ coordination. Ultimately, these three K···O interactions impart an approximate three-fold axis of symmetry in **22** and **23** and preclude the encapsulation of the K^+ ion by 18-crown-6.

3.2. Interactions with Tl^+ cations

Much like K^+, Tl^+ can form interactions with Lewis-basic moieties such as the O and F atoms in an OR^F ligand. While K^+ primarily functions as a Lewis acid due to its noble gas electronic configuration, the filled 6*s* orbital of Tl^+ can also form Lewis-basic interactions with the empty π^* orbitals of arene rings and thallophilic interactions with itself, so-called Menshutkin interactions [57]. Additionally, as a large, electron-rich (soft) metal with high coordination number capacity [58], a single Tl^+ ion can form many Tl···O, Tl···F, Tl···arene, and Tl···Tl interactions within or between M-OR^F complexes.

Two examples of the different structural effects of Tl^+ counter-ions can be seen by comparing two pairs of Co- (**5b** and **13b**) and Cu-containing (**10b** and **17b**) OAr^F and OAr' complexes respectively. As shown in Fig. 4, Co complexes **5b** and **13b** differ in their solid-state nuclearity depending on the aryloxide ligand's interaction with the Tl^+ counter-ions. The OAr^F-containing $[Tl_2Co(OAr^F)_4]$ (**5b**) is monomeric with a single four-coordinate Co center in which each Tl^+ counter-ion bridges two OAr^F ligands; a similar configuration is also observed for Ni-containing **8c** and Zn-containing **11c**. On the other hand, OAr'-containing $[Tl_2Co(OAr')_4]$ (**13b**) forms a solid-state dimer in which the two five-coordinate Co centers are bridged by two OAr' ligands. In this case, these aryloxide ligands are bound in a μ_3-bridging configuration with the two Co centers and a Tl^+ ion, demonstrating the bridging role Tl^+ can play in facilitating the formation of polymeric solid-state structures.

Furthermore, Cu complexes **10b** and **17b** both form multinuclear solid-state structures (Fig. 5) which depend on the bridging interactions of the Tl^+ ions with the OR^F ligand employed as well as the length of the thallophilic interactions formed. Uniquely, OAr^F-containing complex **10b** forms an infinite helical chain in which all aryloxide O atoms bridge between Cu and Tl atoms such that adjacent $\{Cu(OAr^F)_4\}$ units are linked by Tl^+, forming a distorted octahedron of $\{Tl_2(\mu_2\text{-}OAr^F)_4\}$ units which bridge the Cu centers. In this complex, Tl···Tl contacts averaging 3.86(6) Å are also present. On the other hand, OAr'-containing complex **17b** does not adopt an extended helical structure, but is a dimer in the solid

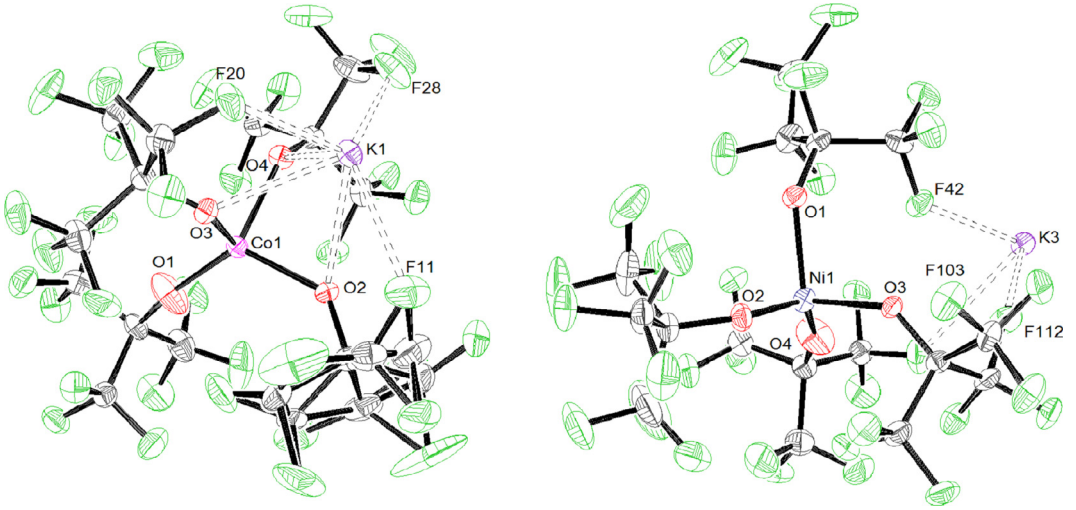

Fig. 3. ORTEP of **22** (left) and **23** (right) showing K···F and K···O interactions. Ellipsoids are shown at 50% probability and $\{K(18C6)\}^+$ cations omitted for clarity.

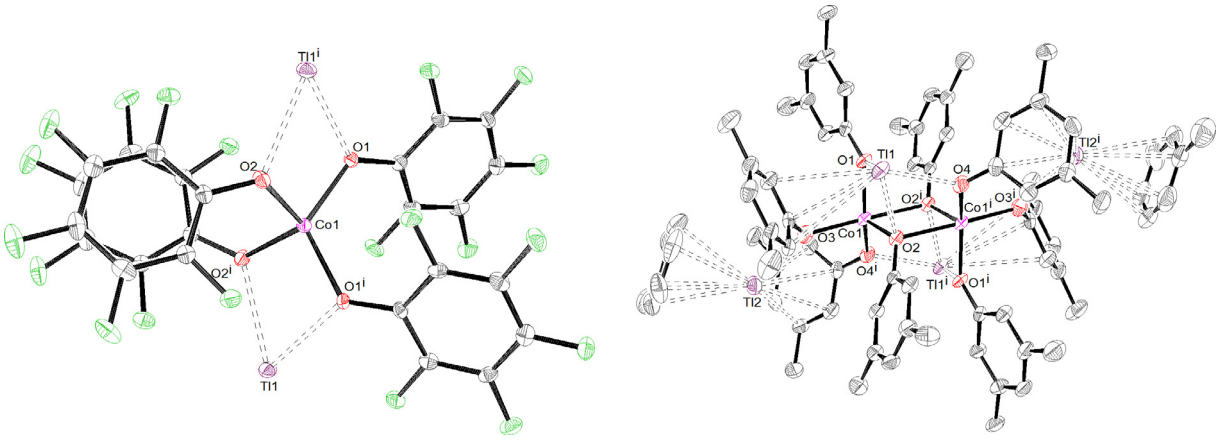

Fig. 4. ORTEPs of Co complexes **5b** (left) and **13b** (right) showing Tl···O interactions with the OAr^F and OAr' ligands. Ellipsoids are shown at 50% probability. H and F atoms omitted for clarity in **13b**.

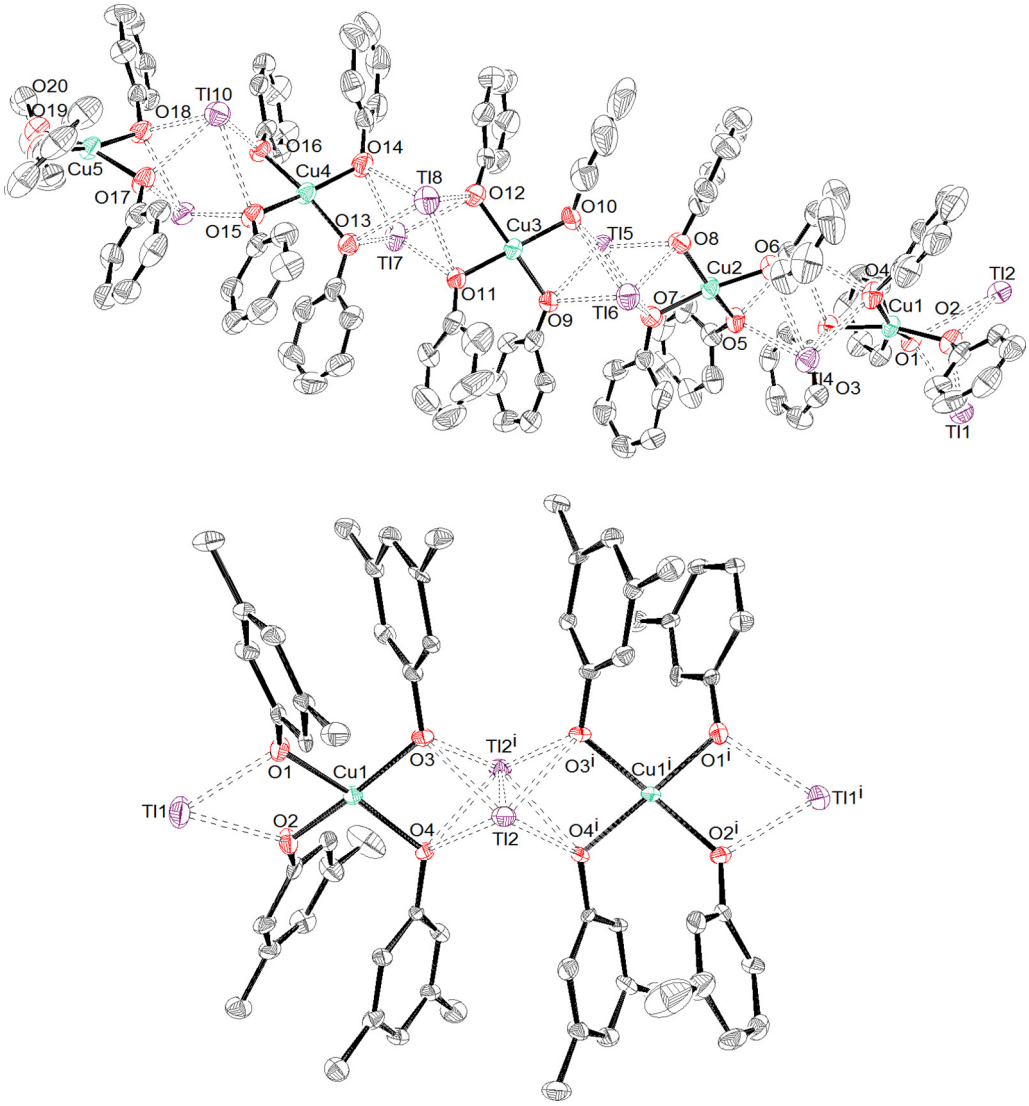

Fig. 5. ORTEPs of Cu complexes **10b** (top) and **17b** (bottom) showing thallophilic and Tl···O interactions with the OAr ligands which affects their nuclearity and structure. Ellipsoids are shown at 50% probability. H and F atoms omitted for clarity.

state with significantly shorter average Tl···Tl contacts of 3.564(1) Å. Due to a lack of π···π stacking between the OAr' arene rings, an infinite chain is not observed for **17b**. However, the formation of solid-state dimer **17b** reveals that the bulkier OAr' ligand does not preclude the formation of bridging $\{Tl_2(\mu_2\text{-}OAr')_4\}$ units. Together, Cu complexes **10b** and **17b** demonstrate the changes in solid-state nuclearity effected by the length of thallophilic interactions and the ligand-dependent Tl···O interactions formed within $[M(OR^F)_n]^{m-}$ complexes.

4. Electronic structure of $[M(OR^F)_n]^{m-}$ complexes

Early experimental and computational work established the ligand field strength of OR^F ligands [43,44]. Comparative spectroscopic analysis of pseudo-halogen $[NiX_4]^{2-}$ (X = NCO, Cl, Br) complexes and Ni-OAr^F, -OAr', and -OC_4F_9 complexes (**8**, **15**, and **23**, respectively) demonstrated that the absorption spectra of Ni-OR^F complexes are significantly blue-shifted versus the halogenated species, indicating a stronger ligand-field than Cl^- or Br^- (Table 3,

Table 3
Electronic spectral data and ligand-field parameters for $[NiX_4]^{2-}$ complexes. Adapted from Zheng et al. [39].

Complex	$E(\nu_3)$ (cm^{-1})	$E(\nu_2)$ (cm^{-1})	B (cm^{-1})	D_q (cm^{-1})	Ref.
$[Ni(NCO)_4]^{2-}$	16 200	9 460	511	311	[60,61]
$[NiCl_4]^{2-}$	14 760	7 470	405	206	[59,61]
$[NiBr_4]^{2-}$	13 320	6 995	379	201	[59,61]
$[Ni(OAr^F)_4]^{2-}$, **8a**	16 660	9 290	877	502	[43]
$[Ni(OAr')_4]^{2-}$, **15**	16 820	10 000	867	540	[43]
$[Ni(OC_4F_9)_4]^{2-}$, **23**	19 300	7 840	1 096	427	[43]

adapted from Zheng, et al.) [43,59–62]. The strongly electron-withdrawing, weak π-donor OR^F ligands are approximately an electronic equivalent to fluoride (F^-), but less prone to bridging, as evidenced by their monomeric structures shown in the structural summary above.

Fluoride ligands stabilize quite high metal oxidation states as in CrF_6, for example, and therefore we hypothesized that these fluorinated alkoxide ligands might likewise support such electronic structures. High oxidation states are also favored by strong σ-donation which can also lead to low-spin configurations. On the other hand, high-spin configurations are promoted by weaker field ligands with extensive π-donor character. Our work revealed that these fluoride-like ligands stabilize relatively high oxidation states *and* high-spin configurations, a rare combination that is of great interest for future reactivity studies. Table 4 provides a broad overview of the electronic structures observed for late first-row $[M(OR^F)_n]^{m-}$ complexes, including examples as predicted (in black) and those that were unexpected (in blue).

All $[M(OR^F)_n]^{m-}$ complexes characterized to date are intermediate or high-spin. While these spin-states are relatively unremarkable for three-coordinate trigonal planar and four-coordinate tetrahedral complexes, high-spin square planar complexes are remarkably rare due to the large energetic separation between the $d_{x^2-y^2}$ orbital and the rest of the *d* orbital manifold. As shown in Table 4, unexpected high-spin configurations (in blue) were achieved in square planar Fe- and Co-pin^F complexes **26b** and **27b.** These compounds are the first and second molecular examples of high-spin square-planar Co and Fe in $\{O_4\}$ coordination, respectively [49], joining a handful of other examples of high-spin square planar Fe(II) [64–75] and Co(II) complexes [69,70,76–80]. Furthermore, in 2018, this chemistry was expanded to include an extraordinary $S = 1$ ground state square planar Co(III) in $\{O_4\}$ coordination, complex **28** [51]. This unique combination of geometry and spin state is made possible by the presence of five non-degenerate *d* orbitals, lack of ligand-based π-acceptor orbitals, and relatively weak ligand field effected by the fluorinated alkoxide ligand.

Reduced π-donation to metal centers means that the ligands are predominantly σ-donors, again favoring higher oxidation states. Indeed, electrochemistry of the $[M^{II}(pin^F)_2]^{2-}$ series with M = Fe (**26b**), Co (**27b**), Ni (**30b**) and Cu (**31c**), shows reversible $M^{II/III}$ couples for Ni and Cu, and quasi-reversible $M^{II/III}$ couples for Fe and Co, respectively (Table 4). Compound **28** is the first trivalent $\{M(pin^F)\}$-containing complex isolated and characterized to date, and other Fe(III) and Cu(III) complexes supported by highly-fluorinated O-donor ligands have prepared as well. The penta-coordinate $[Fe^{III}(OR^F)_5]^{2-}$ with OAr^F (**2a-c**) and OAr' ligands (**12**) are high spin (S = 5/2), whose geometry between trigonal bipyramidal and square pyramidal is subtly cation-dependent [44]. In 2013, oxidative addition via ortho metalation of a partially fluorinated ligand led to the room temperature stable $\{K(18C6)\}[Cu^{III}(OC(C_6H_4)(CF_3)_2)_2]$, featuring hexafluoro-α-cumyl ligands, which is diamagnetic and rigidly planar at the Cu center [63].

Computational analysis of $[M(OR^F)_4]^{2-}$ complexes has supported the qualitative ligand character arguments based on the spectroscopic and magnetic data above [44,49,51]. The reduced π-donor character of fluorinated alkoxide ligands versus their per-protio analogs was demonstrated in a comparison of hypothetical $[Ti^{IV}(OAr)_4]^0$ and $[Fe^{III}(OAr)_4]^-$ [44]. Scheme 9 shows further characteristics and their influence through a series of ligand field splitting diagrams. At the far left, Scheme 9(a) shows the ligand field splitting expected for a square-planar complex with only σ-donation. When some π-donation is added, as in the case of alkoxide ligands, the O *2p* electron contribution into the metal *d* orbitals raises the energy of d_{yz} and d_{xz} in the D_{4h} manifold, as shown in Scheme 9(b) [49]. Furthermore, the observed ligand fields in the $[M(pin^F)_2]^{n-}$ complexes have at most two-fold rotational symmetry due to the reduction in symmetry imposed by the chelate ring. This change removes the degeneracy in the d_{yz} and d_{xz} orbitals, shown in Scheme 9(c), facilitating the S = 1 configuration observed in $[Co^{III}(pin^F)_2]^-$ (**28**) [51].

Current efforts in expanding this chemistry to the middle of the *d*-block (Cr, Mn) and into the earlier metals (Ti, V) may lead to more unusual electronic structures for $\{MO_n\}$ coordination environments.

5. Conclusions and future directions

The collection of over fifty complexes described herein is a significant compendium of late first-row transition metals supported by highly-fluorinated alkoxide and aryloxide (OR^F) ligands. While the corresponding hydro analogs of these ligands often result in extended (μ-OR)-bridged structures, the reduced basicity of OR^F ligands offers an opportunity to access mononuclear metal centers in an all-O-donor environment, although in some cases, reaction conditions can be exploited to isolate dimeric species as well.

Table 4
Observed spin states and $E_{1/2}$ values for $M^{II/III}$ redox couples of $[M(pin^F)_n]^{m-}$ complexes [50]. Spin states depicted in parentheses are observed for similar trivalent $[M(OR^F)_n]^{m-}$ complexes when $[M^{III}(pin^F)_2]^-$ complexes were unavailable for comparison.

	Fe	Co	Ni	Cu	Zn
M^{II}	d^6	d^7	d^8	d^9	d^{10}
	$S = 2$	$S = 3/2$	$S = 0$	$S = 1/2$	$S = 0$
M^{III}	d^5	d^6	d^7	d^8	—
	($S = 5/2$)[44]	$S = 1$	—	($S = 0$)[63]	—
***E*1/2 (V)** vs. Fc/Fc^+	−0.060	0.094	0.356	0.654	—
Compound No.	**26b**	**27b/28**	**30b**	**31c**	**32a**

See above-mentioned references for further information.

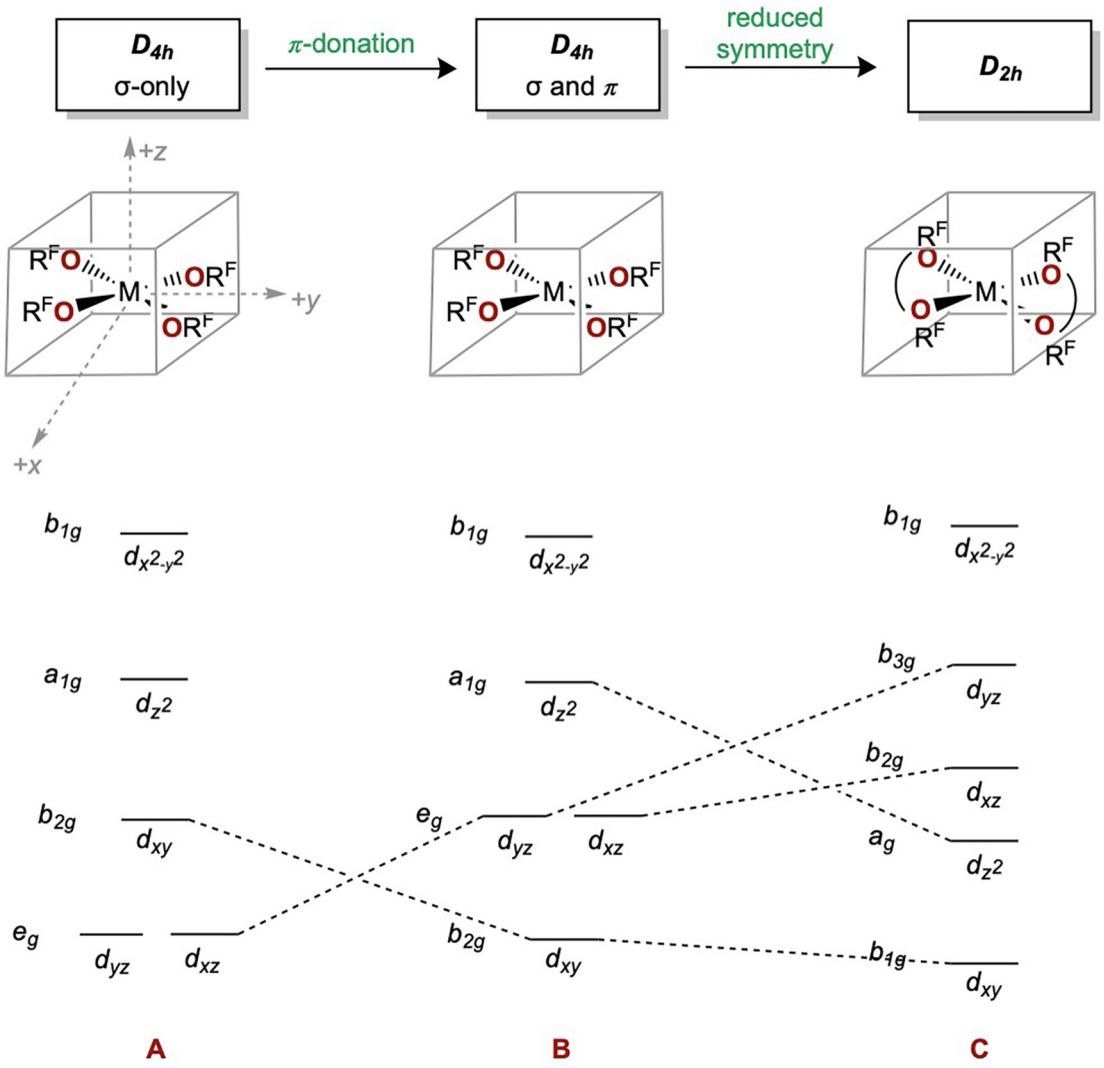

Scheme 9. Qualitative ligand field splitting diagrams for $[M(OR^F)_4]^{2-}$ complexes.

Due to the presence of both O and F atoms on the OR^F backbone, Lewis-acidic counter-ions such as Tl^+ and K^+ can form interactions that influence the solid-state structure and solubility of the resultant complexes. Furthermore, the relatively weak ligand field of these OR^F ligands leads to largely high-spin metal complexes, including several rare examples of Co(II), Co(III), and Fe(II) in high-spin square planar configurations.

While the foundation has been laid in understanding the structure and properties of $[M(OR)_n]^{m-}$ complexes of the late first-row metals, O-donor complexes of the earlier, more oxophilic first-row metals (Sc, Ti, Cr, and Mn) have not been extensively explored, despite their industrial significance. In the realm of perhydro complexes, examples of discrete $[M(OR)_n]^{m-}$ complexes are limited, and many questions remain: What range of oxidation states may be stabilized? What coordination environments and nuclearities might result? What is the air- and water-tolerance of these complexes? Is catalytic potential observed? Looking forward, the preparation of $[M(OR^F)_n]^{m-}$ complexes is a prime opportunity to capitalize upon the advantages offered by fluorinated O-donor ligands in order to fill in this fundamental gap in the chemical literature.

Overall, this summary cohesively and succinctly lays the groundwork in demonstrating the utility and unique properties of transition metal complexes supported by highly-fluorinated O-donor ligands. Having established that unusual electronic structures are possible with OR^F ligands, next, we move forward to expand our body of work to include OR^F complexes of the earlier first-row, heavier *d*-block, and *p*-block metals. Future efforts will significantly expand the reactivity studies to investigate stoichiometric and catalytic oxidative capabilities of these complexes.

Declaration of Competing Interest

The authors declare that they have no known competing financial interests or personal relationships that could have appeared to influence the work reported in this paper.

Acknowledgements

We are grateful to the National Science Foundation (NSF) for support of this work (CHE 01800313 to LHD).

References

[1] S. Paul, F. Neese, D.A. Pantazis, Green Chem. 19 (2017) 2309–2325.

[2] C.W. Cady, R.H. Crabtree, G.W. Brudvig, Coord. Chem. Rev. 252 (2008) 444–455.
[3] S.D. Jackson, J.S.J. Hargreaves, Metal Oxide Catalysis, Wiley, 2008.
[4] B.E.R. Snyder, M.L. Bols, R.A. Schoonheydt, B.F. Sels, E.I. Solomon, Chem. Rev. 118 (2018) 2718–2768.
[5] P. Vanelderen, B.E.R. Snyder, M.-L. Tsai, R.G. Hadt, J. Vancauwenbergh, O. Coussens, R.A. Schoonheydt, B.F. Sels, E.I. Solomon, J. Am. Chem. Soc. 137 (2015) 6383–6392.
[6] S. Grundner, M.A.C. Markovits, G. Li, M. Tromp, E.A. Pidko, E.J.M. Hensen, A. Jentys, M. Sanchez-Sanchez, J.A. Lercher, Nat. Commun. 6 (2015) 7546.
[7] D. Bradley, R.C. Mehrotra, I. Rothwell, A. Singh, Alkoxo and Aryloxo Derivatives of Metals, Elsevier Science, 2001.
[8] A. Grass, D. Wannipurage, R.L. Lord, S. Groysman, Coord. Chem. Rev. 400 (2019) 213044.
[9] J. Hvoslef, H. Hope, B.D. Murray, P.P. Power, Chem. Commun. (1983) 1438–1439.
[10] B.D. Murray, P.P. Power, J. Am. Chem. Soc. 106 (1984) 7011–7015.
[11] B.D. Murray, H. Hope, P.P. Power, J. Am. Chem. Soc. 107 (1985) 169–173.
[12] M.M. Olmstead, P.P. Power, G. Sigel, Inorg. Chem. 25 (1986) 1027–1033.
[13] G.A. Sigel, R.A. Bartlett, D. Decker, M.M. Olmstead, P.P. Power, Inorg. Chem. 26 (1987) 1773–1780.
[14] R.A. Bartlett, J.J. Ellison, P.P. Power, S.C. Shoner, Inorg. Chem. 30 (1991) 2888–2894.
[15] T.V. Lubben, P.T. Wolczanski, G.D. Van Duyne, Organometallics 3 (1984) 977–983.
[16] T.V. Lubben, P.T. Wolczanski, J. Am. Chem. Soc. 109 (1987) 424–435.
[17] P.T. Wolczanski, Polyhedron 14 (1995) 3335–3362.
[18] P.T. Wolczanski, Chem. Commun. (2009) 740–757.
[19] S. Groysman, D. Villagrán, D.G. Nocera, Inorg. Chem. 49 (2010) 10759–10761.
[20] S. Groysman, D. Villagrán, D.E. Freedman, D.G. Nocera, Chem. Commun. 47 (2011) 10242–10244.
[21] M.B. Chambers, S. Groysman, D. Villagrán, D.G. Nocera, Inorg. Chem. 52 (2013) 3159–3169.
[22] R.L. Halbach, D. Gygi, E.D. Bloch, B.L. Anderson, D.G. Nocera, Chem. Sci. 9 (2018) 4524–4528.
[23] J.A. Bellow, D. Fang, N. Kovacevic, P.D. Martin, J. Shearer, G.A. Cisneros, S. Groysman, Chem. Eur. J. 19 (2013) 12225–12228.
[24] M. Yousif, A.C. Cabelof, P.D. Martin, R.L. Lord, S. Groysman, Dalton Trans. 45 (2016) 9794–9804.
[25] J.A. Bellow, M. Yousif, D. Fang, E.G. Kratz, G.A. Cisneros, S. Groysman, Inorg. Chem. 54 (2015) 5624–5633.
[26] M. Yousif, D. Wannipurage, C.D. Huizenga, E. Washnock-Schmid, N.J. Peraino, A. Ozarowski, S.A. Stoian, R.L. Lord, S. Groysman, Inorg. Chem. 57 (2018) 9425–9438.
[27] M. Yousif, D.J. Tjapkes, R.L. Lord, S. Groysman, Organometallics 34 (2015) 5119–5128.
[28] J.F.J. Dippy, R.H. Lewis, J. Chem. Soc. (1936) 644–649.
[29] S. Patai, The Chemistry of the Hydroxyl Group: Part 1, Interscience, London, New York, 1971.
[30] E.V. Dehmlow, R. Thieser, Y. Sasson, R. Neumann, Tetrahedron 42 (1986) 3569–3574.
[31] M.H. Abraham, P.P. Duce, J.J. Morris, P.J. Taylor, J. Chem. Soc., Faraday Trans. 1 (83) (1987) 2867–2881.
[32] C.J. Willis, Coord. Chem. Rev. 88 (1988) 133–202.
[33] E. Parman, L. Toom, S. Selberg, I. Leito, J. Phys. Org. Chem. 32 (2019) e3940.
[34] K.F. Purcell, J.C. Kotz, Inorganic Chemistry, W. B. Saunders, Philadelphia, PA, 1977.
[35] A.P. Purdy, C.F. George, G.A. Brewer, Inorg. Chem. 31 (1992) 2633–2638.
[36] S.C. Cole, M.P. Coles, P.B. Hitchcock, J. Chem. Soc., Dalton Trans. (2002) 4168–4174.
[37] K.J. Weese, R.A. Bartlett, B.D. Murray, M.M. Olmstead, P.R. Power, Inorg. Chem. 26 (1987) 2409–2413.
[38] V.C. Gibson, C. Redshaw, W. Clegg, M.R.J. Elsegood, Polyhedron 16 (1997) 2637–2641.
[39] M.P. Coles, Coord. Chem. Rev. 323 (2016) 52–59.
[40] M.C. Buzzeo, A.H. Iqbal, C.M. Long, D. Millar, S. Patel, M.A. Pellow, S.A. Saddoughi, A.L. Smenton, J.F.C. Turner, J.D. Wadhawan, R.G. Compton, J.A. Golen, A.L. Rheingold, L.H. Doerrer, Inorg. Chem. 43 (2004) 7709–7725.
[41] M.V. Childress, D. Millar, T.M. Alam, K.A. Kreisel, G.P.A. Yap, L.N. Zakharov, J.A. Golen, A.L. Rheingold, L.H. Doerrer, Inorg. Chem. 45 (2006) 3864–3877.
[42] M. Kim, L.N. Zakharov, A.L. Rheingold, L.H. Doerrer, Polyhedron 24 (2005) 1803–1812.
[43] B.N. Zheng, M.O. Miranda, A.G. Di Pasquale, J.A. Golen, A.L. Rheingold, L.H. Doerrer, Inorg. Chem. 48 (2009) 4274–4276.
[44] S.A. Cantalupo, H.E. Ferreira, E. Bataineh, A.J. King, M.V. Petersen, T. Wojtasiewicz, A.G. DiPasquale, A.L. Rheingold, L.H. Doerrer, Inorganic Chem. 50 (2011) 6584–6596.
[45] J.S. Lum, P.E. Chen, A.L. Rheingold, L.H. Doerrer, Polyhedron 58 (2013) 218–228.
[46] M.V. Petersen, A.H. Iqbal, L.N. Zakharov, A.L. Rheingold, L.H. Doerrer, Polyhedron 52 (2013) 276–283.
[47] S.A. Cantalupo, J.S. Lum, M.C. Buzzeo, C. Moore, A.G. Di Pasquale, A.L. Rheingold, L.H. Doerrer, Dalton Trans. 39 (2010) 374–383.
[48] S.E.N. Brazeau, E.E. Norwine, S.F. Hannigan, N. Orth, I. Ivanovic-Burmazovic, D. Rukser, F. Biebl, B. Grimm-Lebsanft, G. Praedel, M. Teubner, M. Rubhausen, P. Liebhauser, T. Rosener, J. Stanek, A. Hoffmann, S. Herres-Pawlis, L.H. Doerrer, Dalton Trans. 48 (2019) 6899–6909.
[49] S.A. Cantalupo, S.R. Fiedler, M.P. Shores, A.L. Rheingold, L.H. Doerrer, Angew. Chem. Int. Ed. 51 (2012) 1000–1005.
[50] L. Tahsini, S.E. Specht, J.S. Lum, J.J.M. Nelson, A.F. Long, J.A. Golen, A.L. Rheingold, L.H. Doerrer, Inorg. Chem. 52 (2013) 14050–14063.
[51] J.L. Steele, L. Tahsini, C. Sun, J.K. Elinburg, C.M. Kotyk, J. McNeely, S.A. Stoian, A. Dragulescu-Andrasi, A. Ozarowski, M. Ozerov, J. Krzystek, J. Telser, J.W. Bacon, J.A. Golen, A.L. Rheingold, L.H. Doerrer, Chem. Commun. 54 (2018) 12045–12048.
[52] S.E.N. Brazeau, L.H. Doerrer, Dalton Trans. 48 (2019) 4759–4768.
[53] L. Yang, D.R. Powell, R.P. Houser, Dalton Trans. (2007) 955–964.
[54] A.W. Addison, T.N. Rao, J. Reedijk, J. van Rijn, G.C. Verschoor, Dalton Trans. (1984) 1349–1356.
[55] J.M. Zadrozny, J. Telser, J.R. Long, Polyhedron 64 (2013) 209–217.
[56] S.E.N. Brazeau, in: Department of Chemistry, Boston University, 2020.
[57] H. Schmidbaur, A. Schier, Organometallics 27 (2008) 2361–2395.
[58] F.A. Cotton, G. Wilkinson, C.A. Murillo, M. Bochmann, Advanced Inorganic Chemistry, 6th ed., John Wiley and Sons, New York, 1999.
[59] F.A. Cotton, D.M.L. Goodgame, M. Goodgame, J. Am. Chem. Soc. 83 (1961) 4690–4699.
[60] D. Forster, D.M.L. Goodgame, J. Chem. Soc. (1964) 2790–2798.
[61] A.B.P. Lever, Inorganic Electronic Spectroscopy, Elsevier, 1984.
[62] A.B.P. Lever, J. Chem. Educ. 45 (1968) 711–712.
[63] S.F. Hannigan, J.S. Lum, J.W. Bacon, C. Moore, J.A. Golen, A.L. Rheingold, L.H. Doerrer, Organometallics 32 (2013) 3429–3436.
[64] S.A. Stoian, J.M. Smith, P.L. Holland, E. Münck, E.L. Bominaar, Inorg. Chem. 47 (2008) 8687–8695.
[65] D. Pinkert, S. Demeshko, F. Schax, B. Braun, F. Meyer, C. Limberg, Angew. Chem. Int. Ed. 52 (2013) 5155–5158.
[66] C.A. Nijhuis, E. Jellema, T.J.J. Sciarone, A. Meetsma, P.H.M. Budzelaar, B. Hessen, Eur. J. Inorg. Chem. 2005 (2005) 2089–2099.
[67] V. Esposito, E. Solari, C. Floriani, N. Re, C. Rizzoli, A. Chiesi-Villa, Inorg. Chem. 39 (2000) 2604–2613.
[68] X. Wurzenberger, H. Piotrowski, P. Klüfers, Angew. Chem. Int. Ed. 50 (2011) 4974–4978.
[69] S. De Angelis, E. Solari, C. Floriani, A. Chiesi-Villa, C. Rizzoli, J. Am. Chem. Soc. 116 (1994) 5702–5713.
[70] J. Jubb, D. Jacoby, C. Floriani, A. Chiesi-Villa, C. Rizzoli, Inorg. Chem. 31 (1992) 1306–1308.
[71] D. Pinkert, M. Keck, S.G. Tabrizi, C. Herwig, F. Beckmann, B. Braun-Cula, M. Kaupp, C. Limberg, Chem. Commun. 53 (2017) 8081–8084.
[72] M.E. Pascualini, S.A. Stoian, A. Ozarowski, K.A. Abboud, A.S. Veige, Inorg. Chem. 55 (2016) 5191–5200.
[73] N. Manicke, S. Hoof, M. Keck, B. Braun-Cula, M. Feist, C. Limberg, Inorg. Chem. 56 (2017) 8554–8561.
[74] S.D. Hallaert, M.L. Bols, P. Vanelderen, R.A. Schoonheydt, B.F. Sels, K. Pierloot, Inorg. Chem. 56 (2017) 10681–10690.
[75] B.M. Hakey, J.M. Darmon, Y. Zhang, J.L. Petersen, C. Milsmann, Inorg. Chem. 58 (2019) 1252–1266.
[76] D. Christodoulou, M.G. Kanatzidis, D. Coucouvanis, Inorg. Chem. 29 (1990) 191–201.
[77] M.E. Pascualini, S.A. Stoian, A. Ozarowski, N.V. Di Russo, A.E. Thuijs, K.A. Abboud, G. Christou, A.S. Veige, Dalton Trans. 44 (2015) 20207–20215.
[78] S.J. Obrey, S.G. Bott, A.R. Barron, Inorg. Chem. 41 (2002) 571–576.
[79] G.H. Spikes, C. Milsmann, E. Bill, T. Weyhermüller, K. Wieghardt, Inorg. Chem. 47 (2008) 11745–11754.
[80] M. Hong, F. Jiang, X. Huang, W. Su, L. Wenjie, R. Cao, H. Liu, Inorg. Chim. Acta 256 (1997) 137–141.